Eur Biophys J (2002) 31: 294–305
DOI 10.1007/s00249-002-0214-6

ARTICLE

Haluk Resat · Maciej Baginski

Ion passage pathways and thermodynamics of the amphotericin B membrane channel

Received: 1 August 2001 / Revised: 14 December 2001 / Accepted: 7 February 2002 / Published online: 13 April 2002

Abstract Amphotericin B is a polyene macrolide antibiotic used to treat systemic fungal infections. Amphotericin B's chemotherapeutic action requires the formation of transmembrane channels, which are known to transmit monovalent ions. We have investigated the ion passage pathways through the pore of a realistic model structure of the channel and computed the associated thermodynamic properties. Our calculations combined the free energy computations using the Poisson equation with a continuum solvent model and the molecular simulations in which solvent molecules were present explicitly. It was found that there are no substantial structural barriers to a single sodium or chloride ion passage. Thermodynamic free energy calculations showed that the path along which the ions prefer to move is off center from the channel's central axis. In accordance with experiments, Monte Carlo molecular simulations established that sodium ions can pass through the pore. When it encounters a chloride anion in the channel, the sodium cation prefers to form a solvent-bridged pair configuration with the anion.

Keywords Molecular simulation · Poisson-Boltzmann equation · Free energy · Ion channel · Ion transport

Introduction

The polyene antibiotic amphotericin B (AmB) (Fig. 1) is one of the leading drugs to treat systemic fungal infections (reviewed in Bolard 1986; Brajtburg et al. 1990; Gallis et al. 1990; Hartsel et al. 1993; WongBeringer et al. 1998). Even though it has severe side effects, AmB is still the most commonly used antifungal drug for the treatment of patients with life-threatening diseases owing to lack of a better alternative (Hartsel and Bolard 1996). In spite of extensive experimental studies carried out over the last 40 years, the mechanism with which AmB interacts with both fungal and mammalian cells is not yet fully understood. Owing to the clinical importance of AmB, comprehensive knowledge of its functional mechanism that would lead to the design of less toxic AmB derivatives (Grzybowska et al. 1997; Cybulska et al. 2000; Resat et al. 2000; Szlinder-Richert et al. 2001) could have a very important medical impact.

It has been proposed that AmB molecules interact with membrane sterols to form transmembrane channels (Andreoli 1973; De Kruijff and Demel 1974; Medoff et al. 1983; Bolard 1986; Brajtburg et al. 1990; Gallis et al. 1990; Joly et al. 1992; Mickus et al. 1992; Hartsel et al. 1993; Weakliem et al. 1995; Hartsel and Bolard 1996; Fujii et al. 1997; Saka and Mita 1998). The channels are responsible for the leakage of monovalent ions, particularly intracellular K^+. This results in the loss of the necessary ionic concentration difference between the cytoplasmic and extracellular sides of the cell membrane, and leads to cell death. The use of AmB in chemotherapy is based on the higher affinity of this antibiotic for ergosterol, the principal sterol in fungal cells, than for cholesterol, the principal sterol in mammalian cells (De Kruijff and Demel 1974; Kotler-Brajtburg et al. 1974; Chen and Bittman 1977; Gruda et al. 1980; Teerlink et al. 1980; Vertut-Croquin et al. 1983; Clejan and Bittman 1985; Gruda and Bolard 1987; Baginski et al. 1989; Herve et al. 1989; Whyte et al. 1989; Jullien et al. 1990; Bolard et al. 1991; Baginski et al. 1994; Langlet et al. 1994; Wolf and Hartsel 1995; Baginski and Borowski 1997; Fournier et al. 1998). Further details of the functioning of the drug may be found in reviews (Bolard 1986; Brajtburg et al. 1990; Gallis et al. 1990; Hartsel et al. 1993).

H. Resat (✉)
Department of Physics, Koç University,
Rumelifeneri Yolu, Sariyer, Istanbul Turkey
E-mail: haluk.resat@pnl.gov

M. Baginski
Department of Pharmaceutical Technology and Biochemistry,
Chemical Faculty, Technical University of Gdansk,
Narutowicza St 11/12, 80-952 Gdansk, Poland

Present address: H. Resat
Pacific Northwest National Laboratory,
P.O. Box 999, Mail Stop K1-83, Richland, WA 99352, USA

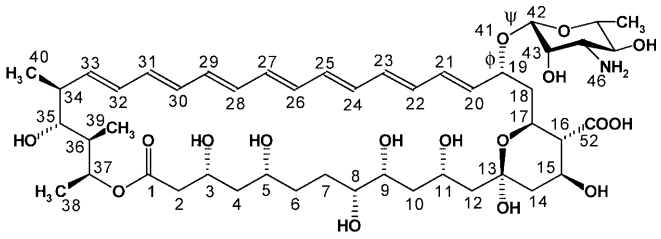

Fig. 1. Molecular structure of amphotericin B. In the text the hydroxyl groups are labeled with the label of the carbon to which they are attached; for example, OH-5 is attached to C5. The orientation of the channel is such that the amino sugar part faces the extracellular side (defined as $+z$), and the tail end of the molecule is towards the cytoplasmic part of the membrane

The exact molecular structure of an AmB channel is not yet known, even though the X-ray structures of AmB and of cholesterol and ergosterol were determined a long time ago (Ganis et al. 1971; Hull and Woolfson 1976; Shieh et al. 1981). Nevertheless, several realistic models of the AmB membrane channel have been proposed and the predicted properties of these channels are highly supported by experimental evidence (Andreoli 1973; De Kruijff and Demel 1974; Van Hoogevest and De Kruijff 1978; Dufourc et al. 1984; Bonilla-Marin et al. 1991; Hartsel et al. 1991; Khutorsky 1992; Balakrishnan and Easwaran 1993; Baginski et al. 1997; Silberstein 1998). In these proposed models, which are very similar, the chain of hydroxyl groups of AmB (Fig. 1) face towards the channel pore, and the conjugated double bond chains are positioned next to the membrane sterols and lipids. Such an orientation of the antibiotic molecules is also supported by recent studies of the amphipatic/amphiphilic pattern of the AmB molecule (Baginski and Borowski 1997) and AmB-like isosterical molecules (DiGiorgio et al. 2000). Additionally, it was found that AmB may form a single length (SLC) or a double length channel (DLC, two SLCs arranged in a tail-to-tail bilayer configuration). It is believed that AmB SLCs are formed when AmB is administered to only one side of the lipid bilayer, and DLCs are formed when AmB is added to both sides of the membrane (Kleinberg and Finkelstein 1984; Bolard et al. 1991; Fujii et al. 1997). Both channels can permeate ions, and depending on the membrane environment (i.e., its lipid content and thickness), and on the availability of AmB, both SLC and DLC types of channels can coexist and function. Since AmB would be administered only from the extracellular side of the cell plasma membrane, it is more likely that only SLCs would be formed under medical usage conditions.

In experiments using artificial black lipid membranes (BLM), SLCs have been observed to have selective permeability to monovalent cations over anions (Andreoli 1973; Marty and Finkelstein 1975; Kleinberg and Finkelstein 1984; Borisova et al. 1986). Moreover, experiments using SLCs formed in small and large unilamellar vesicles showed that the ion selectivity depends on the AmB concentration (Hartsel et al. 1994). Even though a SLC has cation selectivity, the difference between ion permeabilities is not significant and both negatively or positively charged monovalent ions are transmitted through both types of AmB channels at physiological conditions. The reason for the slight ion selectivity is probably the large size of the AmB channel; the pore diameter has been measured to be 7–10 Å, which is larger than the diameter of many protein channels.

In our ongoing efforts to understand the molecular mechanism of the polyene antibiotic AmB, and to find ways to prepare a less toxic drug, we have recently built and tested a molecular model of the AmB/cholesterol channel (Baginski et al. 1997). Our model channel was built by incorporating the known experimental data. In accord with the other AmB model channels proposed and studied by other research groups (Andreoli 1973; De Kruijff and Demel 1974; Van Hoogevest and De Kruijff 1978; Dufourc et al. 1984; Bonilla-Marin et al. 1991; Hartsel et al. 1991; Khutorsky 1992; Balakrishnan and Easwaran 1993), our model AmB channel is constituted of eight AmB and eight cholesterol molecules. We have investigated the stability and molecular properties of our model channel by molecular dynamics simulations, and our findings were in agreement with experiments (Baginski et al. 1997). Building on this earlier study, the present report investigates the ion passage thermodynamics and dynamics of the ions, i.e., passage pathways, within a single length AmB/cholesterol channel. The AmB channel allows for the transport of all small monovalent ions; the investigation of a particular ion is not very important for this channel. Therefore, since they have already been used in previous molecular studies of this channel (Khutorsky 1996), sodium and chloride were chosen as the ions to be investigated in this work.

Our results for the continuum dielectric solvent representation using the Poisson equation show that the passage dynamics of a Na^+ ion should have a diffusional character, i.e., there are no large barriers to its passage. The energy profile for the passage of a Cl^- ion does not have any barriers either and, being almost constant, it implies a passive chloride ion distribution. These results are in agreement with channel conductance experiments. Molecular simulation results showed that the sodium ion can pass through the channel even if an anion is present in the pore. It was observed that the chloride ions sometimes assist the sodium during its passage and that Na^+ and Cl^- prefer to be in a solvent-bridged ion pair configuration while the sodium passes by the chloride. Simulation trajectories showed that the ion paths are quite off center from the channel's central axis and close to the pore surface. This result is also supported by the thermodynamic Poisson equation calculations.

In the following section, we first describe the computational methods and then present results for the thermodynamic free energy calculations, and for the molecular simulations studying the ion motions. We

conclude with a summary and discussion of our findings, any shortcomings of the used methods, and a brief outline of future planned research.

Methods

Channel model

According to the most widely accepted models (Andreoli 1973; De Kruijff and Demel 1974; Khutorsky 1992; Baginski et al. 1997), a conducting AmB channel consists of eight AmB and eight sterol molecules. The pore diameter of these model channels is in accord with the experimental value of 7–10 Å (Holz and Finkelstein 1970). The one-to-one AmB:sterol stoichiometry is also supported by recent experimental observations (Fujii et al. 1997), and theoretical calculations established that such a channel would be stable (Bonilla-Marin et al. 1991; Khutorsky 1996; Silberstein 1998).

The respective lengths of the SLC and DLC are shorter or longer than the membrane thickness. The membrane lipids around the channel arrange themselves so that the length difference is accommodated within the lipid bilayer. A similar lipid arrangement has been observed in the simulation of the gramicidin A channel inserted into a phospholipid bilayer (Woolf and Roux 1996). Another unknown property is what keeps the AmB molecules together once the pore is formed. Since AmB has amino, carboxyl, and many hydroxyl groups (Fig. 1), hydrogen bonding is expected to be the main contributor to the stability of the channel (Herve et al. 1989; Khutorsky 1992, 1996). In our recent study we have observed that there are three intermolecular hydrogen-bond rings (Baginski et al. 1997). The hydrogen bonds between the hydroxyl group OH-8 and either one of the OH-9 or OH-5 groups form a ring and this ring is in the middle part of the channel. The remaining two rings are at the entrance on the extracellular side of the membrane; the first one is between the polar amino and carboxyl groups, and the other is between the OH-15 and OH-43 groups of the sugar moiety. A typical structure of the AmB channel, a snapshot from our previous molecular simulations, is plotted in Fig. 2.

In this work, we choose a sample configuration from an earlier molecular dynamics (MD) simulation (Baginski et al. 1997) as the molecular structure of the AmB channel. The three-dimensional structure of the chosen channel configuration was a good representative of the average structure for the molecular simulation. There are eight AmB molecules interspaced by eight cholesterols in the model channel. The channel has a distorted cylindrical shape (Fig. 2), with a slight twist resembling a barrel where AmB monomers are arranged as staves (Kleinberg and Finkelstein 1984). The channel is tilted by 14° from the normal axis (defined as the z-axis in the remainder of this report) of the membrane slab. The orientation of the channel is such that the amino sugar part faces the extracellular side (defined as $+z$), and the tail end of the AmB molecule is towards the cytoplasmic side of the membrane. For thermodynamics calculations the channel formed by the AmB and cholesterol molecules was immersed into a uniform membrane which was modeled as a low dielectric slab. Similarly, for the Monte Carlo calculations the single channel structure containing explicit cholesterol and lipids was taken from our earlier molecular simulation (further details are given in the "Passage pathways" section below).

Thermodynamics

Since free energy molecular simulations are expensive, the thermodynamics of ion passage was investigated using a continuum dielectric model for the solvating waters using the Poisson equation. The UHBD program (Madura et al. 1995) was used. There have been numerous studies investigating the properties of various membrane channels using a similar approach (Jordan et al. 1989; Partenskii and Jordan 1992; Eisenberg 1996; McGill and Schumaker 1996; Chen et al. 1997; Roux 1997; Sansom et al. 1997; Weetman et al. 1997; Cheng et al. 1998; Kuyucak et al. 1998; Sansom 1998; Laio and Torre 1999; Levitt 1999; Ranatunga et al. 1999; Im et al. 2000; Sansom et al. 2000). In solving the Poisson equation, a dielectric map $\varepsilon(r)$ is created which defines the polarizability of the regions, and the atomic site charges (i.e., the partial charges of AmB and cholesterol atoms) are treated as the free charges ρ^f appearing in the equation:

$$\nabla \cdot \varepsilon(r) \nabla \phi(r) = -\rho^f \tag{1}$$

where $\phi(r)$ is the electrostatic potential. The total electrostatic free energy of a molecular system, ΔG, relative to a reference state in which all the charges are infinitely separated, can be expressed as the sum of two terms (Madura et al. 1995): (1) the free energy of assembling the charges in a uniform dielectric environment, and (2) the solvation (reaction) free energy ΔG^{X} due to the electrostatic potential caused by the polarization of the "solvent" if the dielectric medium is not uniform. The solvation free energy can be calculated after computing the reaction field electrostatic potential (Madura et al. 1995). The overall free energy of placing the ion in the channel then would be found by adding the solvation free energy change upon complex formation and the interaction energy E between the complexing molecules (i.e., between the ion and the channel forming AmBs and sterols) (Madura et al. 1995). Note that this approach does not incorporate the entropic contribution. An entropic correction using the change in the surface areas can be added. Since the molecular surface areas change only slightly with the ion position, the entropic correction would be essentially constant in our case. Therefore, it would not affect the free energy differences and was omitted.

In this study, we have assumed an "interior" dielectric constant of 4 for the channel-forming AmB molecules, for the cholesterols, and for the membrane slab. The solvating regions of the channel pore and both sides of the membrane were assigned a dielectric constant of 78, the dielectric constant of water. Ions were treated as part of the solvated complex and the volume occupied by the ions was also assigned a dielectric constant of 4. As in our earlier study (Baginski et al. 1997), atomic radii values and the other short-range potential parameters for AmB and cholesterol were taken from the

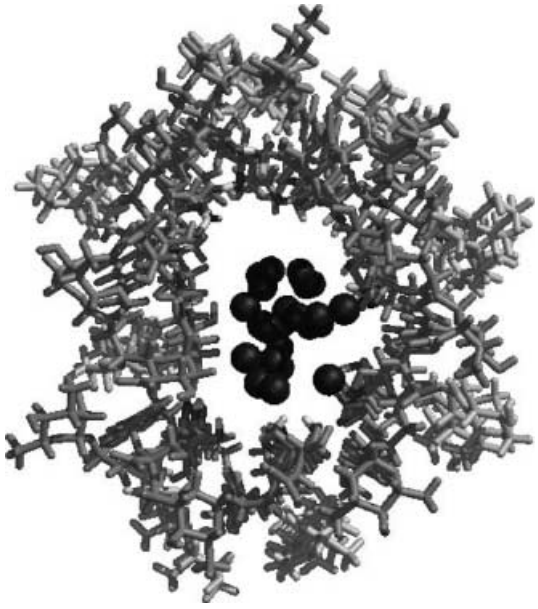

Fig. 2. Top view of the model AmB membrane channel from the extracellular side. For clarity the bilayer phospholipids are not shown. *Dark* and *light shaded* molecules are AmB and cholesterol molecules, respectively. *Spheres* show the lowest free energy path of the sodium ion in the AmB channel as determined from the thermodynamic free energy calculations using the Poisson equation (see the Results/Thermodynamics section)

Charmm force field (Brooks et al. 1983). Similarly, atomic site charges derived by an optimal fit to molecular electrostatic surface potentials were used (Baginski and Borowski 1997). It has been shown that a probe radius of 0.8 Å rather than the commonly used water probe radius of 1.4 Å is more appropriate in studying the properties of polar ligands in confined spaces (Rashin 1989; Resat et al. 1997). Therefore, the molecular surface defining the dielectric interface was formed using a probe radius of 0.8 Å. The calculations employed a 99×99×99 grid and were performed using focusing to a final grid size of 0.4 Å. When present, ions were modeled as spheres carrying full ($\pm e$) electrical charges. Radii of the spheres were 0.95 and 2.21 Å for sodium and chloride, respectively.

Passage pathways

To further investigate the ion passage pathways, one sodium-chloride ion pair was placed inside the pore and Monte Carlo (MC) molecular simulations were performed to follow their motion. Unlike the MD method, the MC method is not deterministic and the generated simulation trajectories do not give any information on the time scale of ion passage through the pore (Friedman 1986; Allen and Tildesley 1987). MC, however, has the advantage over the MD method that, since MC move types and step sizes can be chosen arbitrarily, the trajectories in which the ions pass through the channel can be generated successfully with relative ease.

Starting from different initial coordinates, several trajectories were generated. In these runs, ions showed different types of behavior. To correctly mimic the membrane environment in the simulations, the AmB and cholesterol molecules were placed in a patch of phospholipids. To simplify the MC simulations, channel-forming AmB molecules, cholesterols, and the membrane phospholipids were not allowed to move. In our earlier molecular simulation study (Baginski et al. 1997) the aqueous environment was modeled using a total of 1666 explicit water molecules placed in the pore and on both sides of the membrane channel. Two of the waters were replaced with one sodium and one chloride ion and the remaining 1664 water molecules were used to solvate the channel-membrane complex. Periodic boundary conditions were not used and all molecules were kept within a cylindrical simulation cell using surface constraint forces. Electrochemical driving potential was not included in calculating the forces and the potential energy of the system. Other details of the simulation set up may be found in our earlier paper (Baginski et al. 1997). Before recording the trajectories, the simulated system was equilibrated by constraining the sodium and the chloride ions at their desired initial z-ranges, z_0, using harmonic restraint potentials of the form $U_c = k(z-z_0)^2$. Once the equilibration was achieved, the restraints were removed and the ions were totally free to move.

In the calculations, the Markov chain was generated using the standard Metropolis algorithm, i.e., the ratio of Boltzmann factors before and after each move was compared with a random number in deciding whether to accept or reject a move. The temperature was 298 K. The MC step sizes for ion and water moves were determined by adjusting the acceptance rate to 40%. In each move attempt, an ion was translated up to 0.19 Å in each cartesian coordinate direction using a uniform random sampling. In addition to translating with uniform sampling of up to 0.57 Å in each direction, the water molecules were also rotated randomly up to 50°. A preferential sampling whcih selects the waters within the pore more often than those outside was employed. This allowed for obtaining better statistics for the waters in the pore. To improve the sampling of ion movements, one in every ten moves was chosen as an ion move. Since MC simulations do not reveal the temporal information directly, the choice of run lengths in MC simulations is in general somewhat arbitrary. As our main objective was to study the mobility of the ions, reported simulation runs were stopped either when the ions had gone through an interesting motion (such as passing by each other) or when the obtained configuration was judged to be uninteresting (for example, ions move away from each other and lose their ion-pair configuration). This stopping criterion led to runs with different simulation lengths. It should be noted that the use of a rigid channel might have an effect on the motion of the waters and the ions within the pore. However, since AmB channel has a large size and the polar interactions are not very strong, employment of a rigid pore is not expected to have a major effect on the mobility of the waters and the ions. Even if the water and ion motions may be affected, it should be stressed that this would mainly change the transport rates and would not considerably alter the thermodynamic results. Our primary interest in this work is not the determination of the transport rates; therefore, the use of a rigid channel does not introduce errors that would alter our conclusions. The range of the molecular motions in the simulations was observed to be reasonably large. This observation also supports the point that keeping the channel rigid did not have any important effect on the ionic motion in the pore.

In all runs the initial chloride position was around the OH-3 group. The sodium was placed in the vicinity to the extracellular side of the chloride. The lengths of the trajectories of the four runs that are reported were 85, 290, 100, and 110 million moves. In an aqueous environment, Na^+ and Cl^- ions can form either a contact or a solvent-separated pair configuration (Pratt et al. 1994). Here, the contact pair refers to the configuration where the ion separation distance is less than 3 Å and there are no bridging waters between the ions. In the solvent-separated pair configuration, one (or more) water molecule bridges the ions, and the distance between the ions is about 4.5 Å or more.

In the first run, the sodium was initially placed at the level of the OH-5 group and was in a solvent-separated pair configuration. In the second run, the sodium was pulled away from the chloride ion and was placed at the level of the C6 and C7 carbons (Fig. 1). The third run was similar to the first run, but this time the chloride ion was pulled towards the sodium. In the last run, both ions were at the level of the OH-3 groups, and they were in a contact pair configuration. It should be noted that, if there is a constriction region, it is expected to be formed by the OH-5, C6-C7, and OH-8 groups which separate the wide entrance region from the narrow tail part (Khutorsky 1996). Also notice that the molecular simulations performed in this work assume that the cation is already halfway through the channel. Studying the whole trajectory of the ions could be very illuminating; however, such computations are very expensive. Therefore, only the passage of the cation through the part of the channel around the expected constriction zone was investigated in this study.

Results

Thermodynamics

Cation in the pore

The ion locations used to calculate the free energies pathway were chosen as the positions of the oxygens and the hydrogens of the waters. In other words, the pore waters of the selected MD configuration were determined, and there were 145 such waters. The ion placement sites were then chosen as the locations of the oxygens and the hydrogens of these 145 pore waters. The Poisson equation was solved 435 times, each time by placing a Na^+ cation in one of the picked sites and treating the rest of water molecules as a continuum medium. During this placement the channel structure was kept fixed, i.e., possible structural changes due to the placement of an ion in the vicinity of channel molecules were assumed to be negligible. To test whether this was a plausible assumption, we have also chosen 14 configurations in which the cation was next to one of the hydroxyl groups and energy minimized the structures.

During the energy minimization, pore waters were explicitly included and there were no constraints on the movement of the cations, the waters, or the AmB hydroxyl groups. The macrolide rings part of the AmBs and the cholesterol molecules were not allowed to move. The structures used in the Poisson calculations were later obtained by removing the waters from the minimum energy configurations. As the results given in Fig. 3 show, there is no noticeable difference between the energy-minimized and the fixed-structure free energy results. Therefore, in the rest of the calculations, no further energy minimization was employed. Note that Fig. 3 shows the free energy of the complex (also called the potential of mean force W when calculated as a function of coordinates) defined as AmBs, cholesterols, and the pore ion. Therefore, the reported values (ca. 195 kcal/mol) are different from that of an ion (ca. 100 kcal/mol).

Figure 3 shows all 449 points (435 chosen locations plus 14 energy-minimized structures) at which the free energies were calculated. Since the objects will move along the lowest possible energy values on a free energy surface, only the configurations with low free energies are the physically relevant ones. Therefore, in the remaining figures (Figs. 4, 5, 6), only the results for configurations with the lowest free energies at each z-value along the pore axis are given. These configurations are highlighted in Fig. 3. Omitted points are the irrelevant results due to the arbitrarily picked ion positions. Note that, since the important physical quantity is the difference between the free energies, the absolute values of the reported results can be shifted by a constant value without affecting the deduced conclusions (Friedman 1986). The results in Fig. 4 were obtained by shifting the results of Fig. 3.

As Fig. 4 reveals, the channel introduces a small structural free energy barrier of about 1.5 kcal/mol to a single sodium ion passage through the pore. In a physiological environment the electrolyte concentration difference between the two sides of the membrane and the membrane potential give rise to an electrochemical driving potential (Hille 1992; Sperelakis 1995). This driving potential was not included in the Poisson-Boltzmann equation calculations. Our results for a single ion, however, can be modified to mimic the

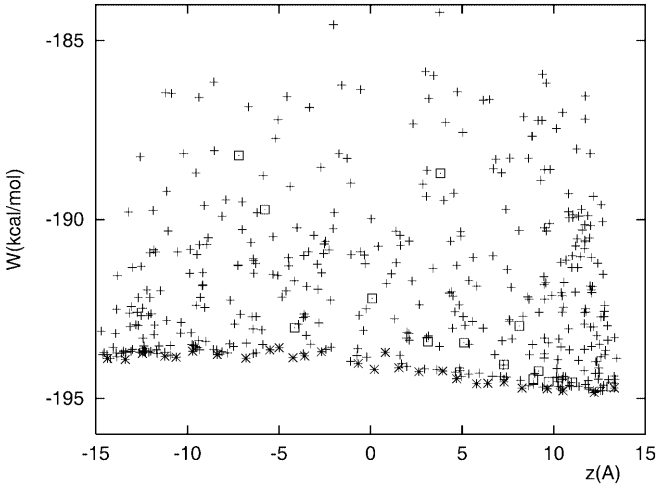

Fig. 3. The free energy of forming a transmembrane AmB-cholesterol channel in a dielectric medium with a dieletric constant of 78 and placing a sodium ion in the pore. The free energy is calculated using the Poisson equation. *Square* and *plus signs* show the results for the channel structures with and without optimizing the orientations of the hydroxyl groups, respectively (see the text). *Crosses* show the results with the lowest free energies; these are the points used in later analysis

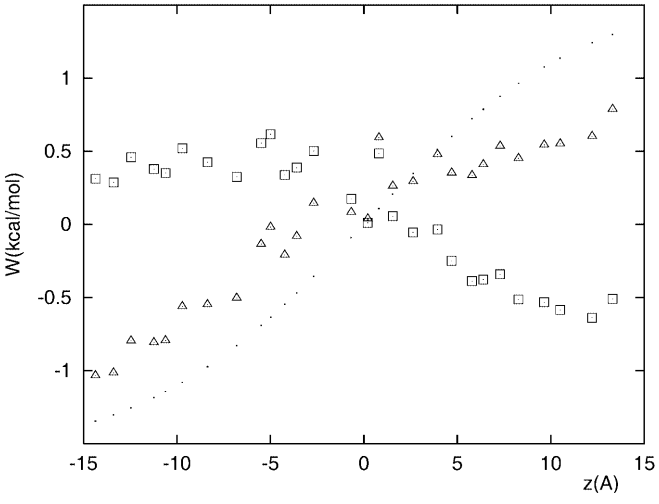

Fig. 4. The potential of mean force of a single sodium ion in the AmB channel. The *square* and *triangle signs* show the results without the electrochemical driving potential and with a –140 meV electrochemical driving potential, respectively. The electrochemical driving potential (*dotted line*) was added as a hyperbolic function: $V_m = 1.62 \tanh(z/12)$ kcal/mol

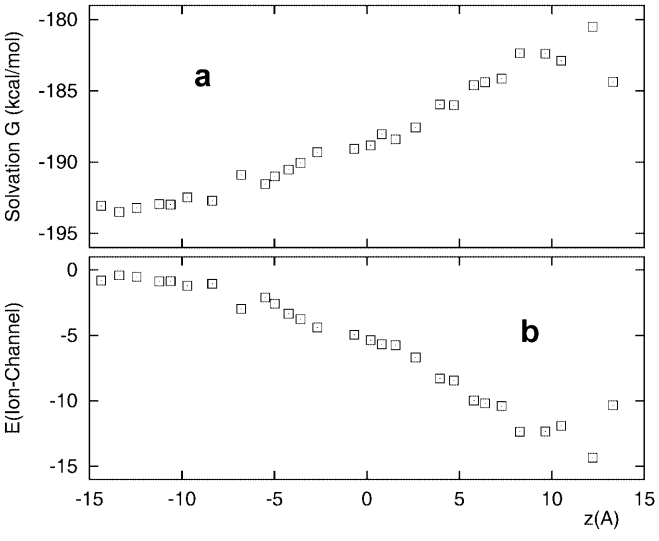

Fig. 5. Components of the free energy of a single sodium ion in the AmB channel: **a** the solvation free energy of the AmB-cholesterol-ion complex, and **b** the electrostatic interaction between the sodium and the channel molecules

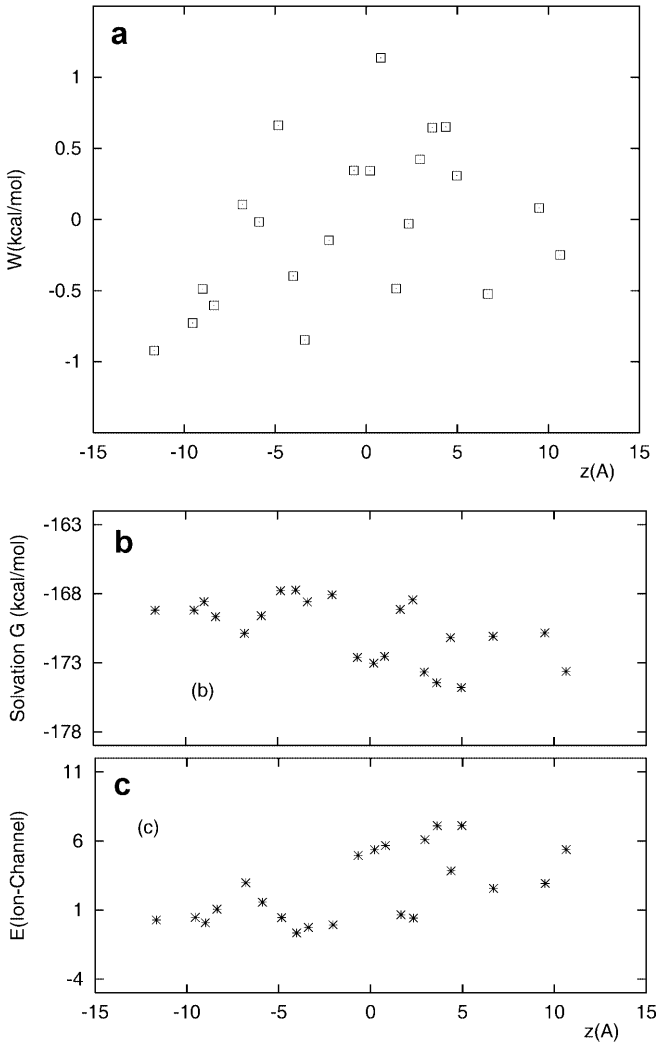

Fig. 6. **a** The potential of mean force of a single chloride ion in the AmB-cholesterol channel. **b** The solvation free energy of the AmB-cholesterol-chloride complex. **c** The electrostatic interaction energy between the chloride and the channel molecules

physiological situation by adding the driving potential across the membrane to the computed free energies. It should be noted that this treatment assumes that different contributions to the free energies are additive. Even though its validity cannot be proven, the additive free energy assumption is expected to be reasonable. Under physiological conditions, cytoplasmic and extracellular sodium concentrations are usually 15 and 145 mM, respectively. Using the Nernst equation at 37 °C and a membrane potential of –80 mV, the electrochemical driving potential for the sodium ion can be estimated as 140 meV = 3.23 kcal/mol (Hille 1992; Sperelakis 1995). This potential is directed to bring about a net inward (i.e., from the extracellular to cytoplasmic side) flow of Na^+. Thus, the electrochemical driving potential is slightly larger than the structural free energy difference between both sides of the membrane. Since the electrochemical driving potential dominates, there are no significant structural barriers (Fig. 4). Sodium ions would move from the extracellular side to the cytoplasm by diffusing, and their flow will be in the direction favored by the free energy gradient. This implies that the AmB channel is not a pump but is in fact an ion channel. It should be emphasized again, however, that our conclusions are based on the results obtained for our model channel with the additional assumption that the errors involved in the computations are smaller than the observed trends. Although there is no unique way of assigning error bars to our results, we estimate them to be small enough (~1 kcal/mol) not to alter our conclusions. This confidence level was determined by taking into account the fact that the free energy profile is determined by comparing the values obtained for different ion positions. Therefore, since differences in the free energy values are calculated, the associated errors tend to cancel. This is a common assumption in many types of free energy difference calculations.

A noticeable result (Fig. 5) is that the observed small structural barrier is the result of two large opposing contributions: the free energy due to the loss of water solvation, ΔG^X, and the coulombic interaction energy, E, between the ion and AmB and cholesterol molecules. This observation is actually to be expected because the pore surface has many hydroxyl or other polar groups that can be used by the ion to replace the polar interactions lost due to stripped-off waters. In calculating the ion-channel interaction energy, short-range (i.e., Lennard-Jones potential) interactions were not included because they make a relatively constant contribution along the minimum free energy path; thus, they would not have any significant effect on the potential of mean force (pmf).

Another relevant question is the path of ion passage through the channel. Closer inspection of the possible path of a sodium ion defined using the pmf (Fig. 4), and shown in Fig. 2, reveals that the path of the ion is continuous. The AmB channel is large enough that small ions can pass through while keeping their solvation shells. In such a case, the ion would be expected to stay close to the center axis of the channel. However, inspection of the locations with low free energies shows that the sodium ion favors following a path which is away from the channel's center axis. This result is in accord with Khutorsky's findings (Khutorsky 1996) and, as discussed later, is further supported by our molecular simulation studies. As mentioned above, there are many hydroxyl groups residing on the channel surface. These groups can replace the ion's first hydration shell waters without significant energy or entropy costs. Owing to such possible polar interactions with the channel, staying close to the pore surface while passing through the channel can be a more favorable path.

Anion in the pore

Experiments have shown that the AmB channel has an interesting selectivity property; depending on the form

of the channel, i.e., whether it is SLC or DLC, it is either cation or anion selective (Andreoli 1973; Marty and Finkelstein 1975; Kleinberg and Finkelstein 1984). Therefore, the thermodynamics of a chloride anion in the channel was also investigated. The free energy profile of the chloride ion in the pore was calculated using the approach described above for the cation case, except that a chloride ion rather than sodium was placed in various places in the pore.

As Fig. 6a shows, as in the cation case, there are no apparent strong binding sites for the chloride in the pore. Note that, in many types of cells, Cl^- is not actively transported; therefore, chloride is distributed passively. This means that the electrochemical driving potential for chloride approximately vanishes (Hille 1992; Sperelakis 1995). Our results (Fig. 6) predict that there is no barrier to the chloride passage through the channel and that the pmf of a chloride ion in the pore is almost constant. There is no trend larger than the fluctuations observed in the pmf profile, ~0.5 kcal/mol, in these results that can be used to derive additional physiological conclusions. Thus, in accord with experiments, the channel does not significantly disturb the equilibrium distribution of the chloride and it would be expected that Cl^- would be passively distributed across the membrane. When the pmf is separated into solvation and direct interaction terms (Fig. 6b and c), we observe that there is a cancellation between these two contributions. However, contrary to the sodium ion case, the change in each term as a function of the chloride ion position is much less severe. Note that, if the ions were to be placed in the same position, the electrostatic interaction energy between the channel forming molecules and a cation or anion would be equal in magnitude but opposite in sign. In this respect Figs. 6c and 5b may look wrong. However, in our calculations the ions are allowed to occupy their most favorable locations, i.e., the lowest free energy positions, along the channel. Therefore, at a certain z-level along the channel, the favorable x-y locations may not be same for an anion and a cation. Actually one would expect to get different locations for oppositely charged ions. For this reason, one would expect to obtain different electrostatic interactions between a cation or an anion and the channel molecules. This is reflected in our results reported in Figs. 6c and 5b. What is important is that, for oppositely charged ions, the electrostatic interaction energies and the solvation free energies increase in reverse directions along the channel. Another trend noteworthy to mention is that these two energy terms tend to cancel each other for both ion types.

Implications for selectivity

Even though we have not investigated potassium ion passage, based on the results reported in Fig. 4 it can be predicted that the free energy profile for the potassium ion will be in accord with the experiments. Since they have similar sizes, one can presume that solvation free energy of a potassium ion in the pore will be similar to that of a sodium ion, i.e., the solvation free energy would give rise to an approximately 1.5 kcal/mol structural barrier. At physiological conditions, the electrochemical driving potential of the potassium is about $+14$ meV $= 0.32$ kcal/mol directed outwards (Sperelakis 1995). Addition of these two contributions would result in a free energy difference that is approximately 1.8 kcal/mol lower on the extracellular side of the membrane. The total pmf for K^+ in the channel would be a simple sloped curve predicting that the potassium ions would flow out of the cell. Thus, the channel would allow potassium ions to leak out of the cell, disrupting the required potassium gradient. This mechanism is the accepted function of the drug (see, for example, Bolard 1986). Since the response of the K^+ ion is based on inference from the Na^+ ion results, given sizable error bars in the results, it should be considered with caution.

Our results are in good agreement with the experiments showing that SLCs have selective permeability to monovalent cations over anions (Marty and Finkelstein 1975; Kleinberg and Finkelstein 1984). As reported above, calculated free energies of transport (ca. 1.5–2 kcal/mol for both sodium and potassium ions) could explain what would happen in physiological situations: sodium ions would be transmitted to the cytoplasm and potassium ions would leak out of the cell. In contrast, the free energy profile for a chloride ion is approximately constant, thus giving a passive distribution. Therefore, the channel is expected to favor the transport of cations over anions.

Ion mobility in the channel and ion passage pathways

Investigation of the MC simulation trajectories (Figs. 7, 8, 9, 10) reveals several interesting observations. In the first run (Fig. 7), the chloride ion hardly moves. The sodium ion is to the extracellular side of the anion at the beginning. While passing by the anion, the sodium first moves along the pore axis and during this movement the ions stay in a solvent-separated pair configuration (Fig. 7a and b). When sodium reaches about the same z-level of the anion, it moves to the side and passes through the constriction. During this passage, ions break loose from the solvent-separated configuration, and the cation diffuses away towards the cytoplasmic side.

Compared to the first run, in the second run (Fig. 8) the sodium was pulled away from the anion at the start. This changed the trajectory considerably. This time the cation does not move much; the anion, however, moves back and forth between its initial location and the tail end of the pore. The ions did not form a paired configuration during the run.

In the third run (Fig. 9) the anion was brought closer to the region between the OH-3 and OH-5 groups, and it was closer to the former OH moiety. The sodium was

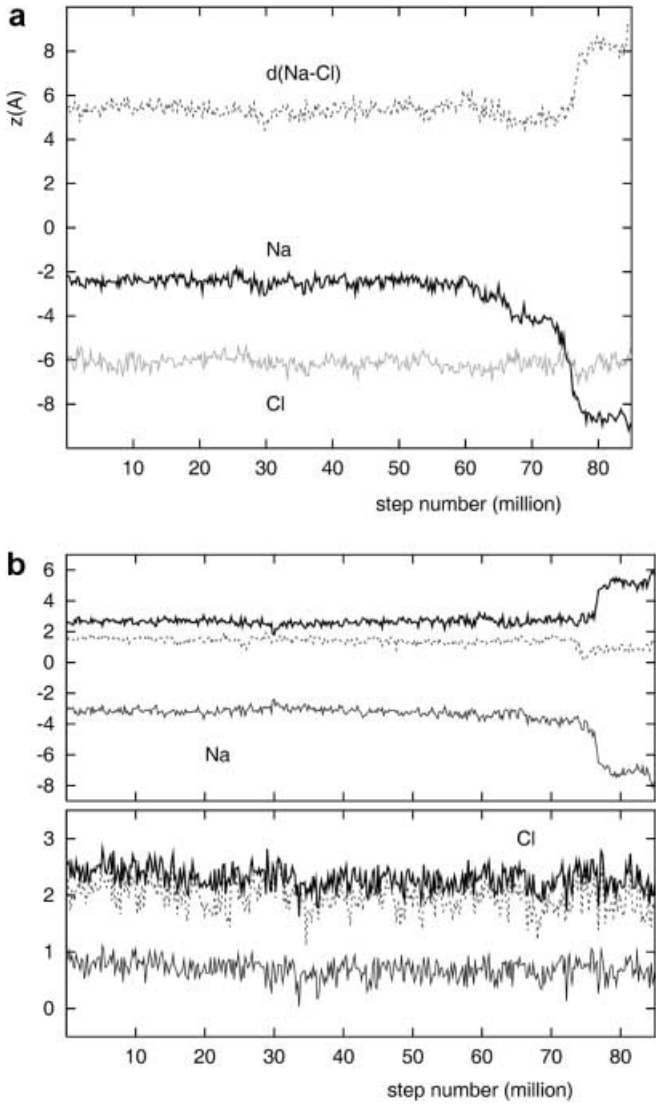

Fig. 7. **a** Monte Carlo simulation trajectory of the ions along the channel's normal axis z. *Dark* and *light solid lines* are for the sodium and the chloride ions, respectively. The *dashed line* shows the distance between the ions. **b** Motion of the sodium and the chloride ions in the x-y membrane plane. The *dark solid line* shows the distance of the ion from the central channel axis. The *light solid* and *dashed lines* are the x and the y coordinates, respectively. All distances are in ångstroms, and the horizontal coordinate is the simulation time in millions of moves

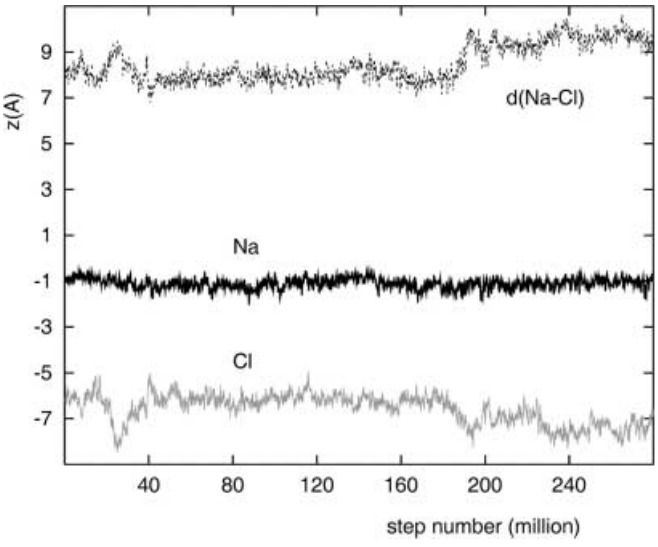

Fig. 8. Same as Fig. 7a but for the second simulation run (see the text)

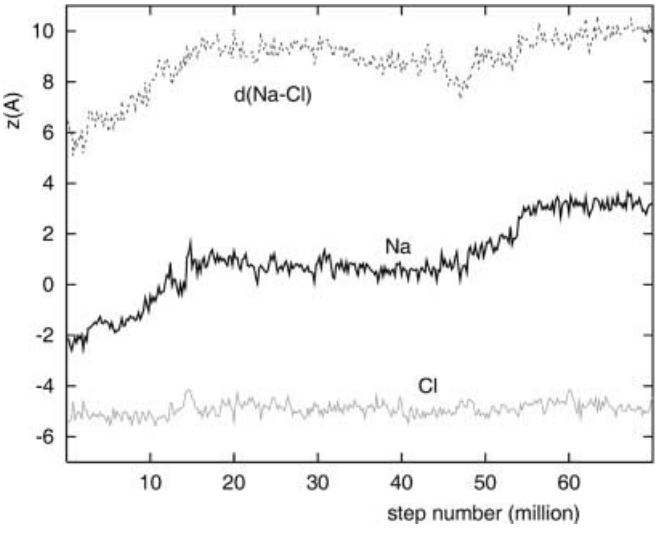

Fig. 9. Same as Fig. 7a but for the third simulation run

placed at a solvent-separated ion pair configuration and was at the OH-5 group level. During the run the anion kept its z-level, but the cation moved away from the anion toward the C6-C7 constriction region separating the wide and the narrow parts of the pore.

In the fourth run (Fig. 10), ions initially were in a contact pair form. During the run, the sodium first moves to the same z-level of the chloride ion and finds itself a stable position. During this time, the ions go from the ion-pair to the solvent-bridged configuration. The ions then fluctuate at this z-level (in between the OH-3 hydroxyl and $C_1=O$ carbonyl groups) for some time as a solvent-separated pair. Then, the chloride ion breaks loose, diffuses away, and leaves the channel through the tail end.

Even though the reported trajectories are only a few of the many possible ones, and by no means form a complete statistical set, they are very illuminating (a complete study with satisfactory statistics would require at least thousands of trajectories). They, however, clearly show that the ions can be quite mobile in the pore. The runs also show that it is possible for the sodium to pass by the chloride ion (as in the first run) when the latter is next to the OH-3 groups. Similarly, the motion of the chloride is not considerably hindered by the channel, or by the sodium either. Although it exited the channel in the fourth run, and was quite mobile in the second run, the region around the OH-3 groups seems to be a stable (probably a metastable) location for the

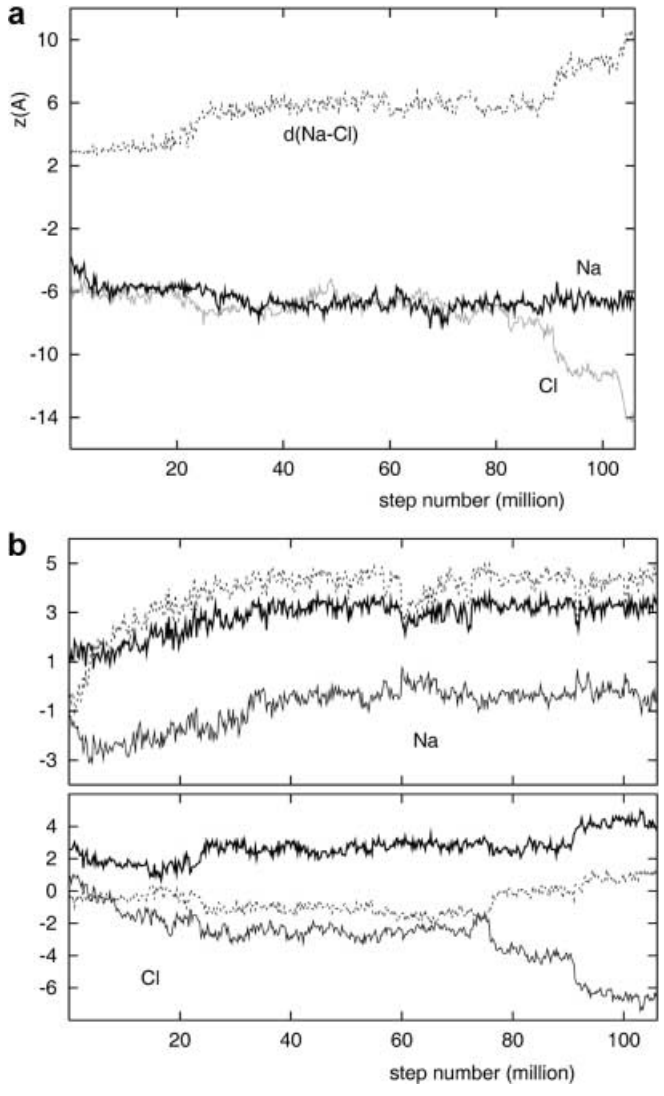

Fig. 10. Parts **a** and **b** are the same as Fig. 7a and b, respectively, but for the fourth simulation run

chloride. While nearby, the sodium seems to favor to be in a solvent-separated pair configuration with the anion. Note that, compared to a contact-pair configuration, being in a solvent-separated pair configuration would lower the dielectric friction on the sodium owing to the anion's field. Thus, the solvent-separated configuration should have a smaller barrier towards the cation passage; observed trajectories actually confirm this expectation. A common outcome of all four runs is that rather than coming closer, the sodium and the chloride tend to separate. This finding implies that the ions do not favor pair formation and prefer to move independently, as they would in bulk solution.

Discussion

Using realistic structures supported by experiments, we have investigated the ion passage pathways and thermodynamics through the AmB channel. This study consisted of two parts and combined the techniques of continuum solvent representation to determine the thermodynamic properties using the Poisson equation and Monte Carlo molecular simulations for the passage pathways where waters were included as explicit molecules.

In the thermodynamic free energy calculations using the Poisson equation with the dielectric continuum solvent representation, it was found that there are no substantial structural barriers to either the sodium or the chloride ions when only one ion is present in the channel. The form of the Poisson (-Boltzmann) equation used here does not actually match the studied system. This is due to the fact that, under physiological conditions, the channel and the membrane system are in an aqueous environment with non-zero electrolyte ion strength. Also the ion compositions on the cytoplasmic and extracellular sides of the membrane are different and, combined with the membrane potential, this ionic concentration difference gives rise to an electrochemical driving potential across the membrane (Hille 1992; Sperelakis 1995). In our work, the simplifying assumption was made by setting the ionic strength to zero on both sides of the membrane in the Poisson equation calculations and the electrochemical potential was added at the end as a correction. Setting the ionic strength to zero causes the omission of the Debye-Hückel screening effect from the computations. An ideal calculation should incorporate these environmental conditions into the equations and should also allow for a flexible channel structure. An approach recently developed by Roux (1997, 1999) can prove to be useful for this purpose. However, the error associated with neglecting the physiological electrolyte salts from the Poisson-Boltzmann equation is quite small and should not alter the conclusions of this report. When it becomes computationally feasible in the future, much more expensive approaches, such as the explicit water grand canonical ensemble free energy molecular simulations (Resat and Mezei 1994; Resat et al. 1997), would be more reliable for the calculation of the thermodynamic properties of the investigated channel.

Since the AmB channel has a diameter large enough to accommodate the small ions with their complete solvation shell, one immediate question is whether the ions pass through the channel while staying close to the center axis of the pore. Both the pmf calculations using the Poisson equation with a continuum solvent and the explicit water MC molecular simulation studies showed that the sodium and chloride ions both prefer to be close to the pore surface and off center from the channel's central axis. Since there many AmB hydroxyl groups residing at the pore surface, when ions are close to the pore surface, these hydroxyl groups can substitute for the lost solvating water molecules without any substantial energy cost.

MC molecular simulation studies investigating the sodium passage pathways showed that a chloride anion

initially placed at a likely position in the pore does not stop the passage of the sodium ion. Similarly, the existence of the sodium does not hinder the movement of the anion, and the chloride was observed to be able to move considerably inside the pore. This observation is again consistent with the experiments that the channel is not strongly cation or anion selective. A configuration common in the simulations was that while the sodium is near the chloride, the ions prefer to be in a solvent-bridged pair form. This configuration should be preferable because it lowers the dielectric friction on the sodium ion and makes it easier to break loose from the chloride after the ions trade places along the *z*-axis. The observation that the sodium-chloride pair prefers to form a solvent-bridged pair is in accord with the Na-Cl pmf results in aqueous solutions (Pratt et al. 1994), which predicts that the ion-contact pair is less stable than the solvent-bridged configuration. In the long run, however, the ions tend to separate and act as in bulk aqueous solution, implying that the solvent-bridged or the contact-pair configurations are only metastable.

The conductance of a single AmB channel is considerably lower than what is expected from an ion channel with such a large diameter. The low conductance of the AmB channel implies that the *effective* pore diameter is smaller than 7–10 Å and this can be explained with the structural properties of the channel. The channel-forming AmB and sterols are not covalently bonded, which makes the AmB channel more fluid along the membrane plane (Kasumov et al. 1979; Brutyan and McPhie 1996). Such lateral fluidity would introduce frequent deformations in the channel structure, making the smallest cross-section area, and the corresponding effective diameter, smaller than its static value. This reduction in the pore dimensions can be the reason for the low conductivity. The time scale associated with the lateral movements of the channel is much longer than the time scale of typical simulations; therefore, it would not be possible to investigate such motions using molecular modeling approaches. However, it was observed in our previous MD study that the shape of the channel becomes deformed from a cylinder to that of an ellipsoid, implying that the channel has a lateral mobility (Baginski et al. 1997).

A recent study on hypothetical model ion channels established that the free energy profile of ions in the pore is sensitive to the value of the dielectric constant of the channel water used in the Poisson equation calculations (Weetman et al. 1997). It was found in this study that, in general, the barrier to ion passage becomes larger as the value of the pore dielectric constant is reduced. In this study we have not tried different dielectric constants for the pore waters. The dielectric constant chosen was that of the bulk water. There were two structural reasons for this choice: (1) the pore is large enough to accommodate several water molecules at the same *z*-level, and (2) the pore surface is lined up with hydroxyl groups of AmB molecules. Thus, there is enough room so that the movements of the pore water molecules are not severely hindered, and the hydroxyl groups create an environment resembling that of the bulk by allowing for hydrogen bond substitution. For these reasons, we expect the dielectric constant of the pore waters in the AmB channel to be very close to the bulk water dielectric constant. This expectation, however, needs to be tested by calculating the dielectric constant of the pore waters using molecular simulations.

Complementary studies for the potassium ion and for the ergosterol membrane channel are expected to point out the slight activity difference of the AmB antibiotic for the ergosterol- and cholesterol-containing membranes. These studies will be undertaken after obtaining sample channel structures from the molecular simulation of the AmB channel in an ergosterol-containing membrane, and such molecular simulations are currently underway in our group.

We would like to add a cautionary note that the channel investigated in this study is a model channel built by making use of the available experimental information to the full extent possible. The question of how realistic the model channel is can only be answered unambiguously when the structure of the AmB channel is determined. In this respect, the results of this work should be considered in conjunction with the model structure used, and the model should be further tested as new experimental evidence becomes available. However, in this and in our earlier work, we have shown that our model successfully explains the currently available experimental data.

At the end it is worth noting that, because of its large diameter, the AmB channel differs from many other membrane protein channels with narrow pores (e.g., gramicidin A channel). Therefore, computational methods utilized in the rather extensive studies of ion permeation in gramicidin channels, and the findings of those studies, are not directly comparable to our work. On the other hand, the AmB pore can be a good system to study molecular properties of wide channels formed by association of independent building blocks. In this respect, our present study also tested some of the available theoretical methods in studying ion passage through wide membrane channels.

Acknowledgements This work was partially supported by The State Committee of Scientific Research, Warsaw (Poland) (grant number 3T09A07014). We would like to thank Dr. B. Cybulska for her assistance and helpful comments.

References

Allen MP, Tildesley DJ (1987) Computer simulation of liquids. Oxford University Press, New York

Andreoli TE (1973) On the anatomy of amphotericin B-cholesterol pores in lipid bilayer membranes. Kidney Int 4:337–345

Baginski M, Borowski E (1997) Distribution of electrostatic potential around amphotericin B and its membrane targets. Theochem J Mol Struct 389:139–146

Baginski M, Tempczyk A, Borowski E (1989) Comparative conformational analysis of cholesterol and ergosterol by molecular mechanics. Eur Biophys J 17:159–166

Baginski M, Bruni P, Borowski E (1994) Comparative analysis of the distribution of the molecular electrostatic potential for cholesterol and ergosterol. Theochem J Mol Struct 311:285–296

Baginski M, Resat H, McCammon JA (1997) Molecular properties of amphotericin B membrane channel: a molecular dynamics simulation. Mol Pharmacol 52:560–570

Balakrishnan AR, Easwaran KRK (1993) Lipid-amphotericin B complex structure in solution – a possible first step in the aggregation process in cell membranes. Biochemistry 32:4139–4144

Bolard J (1986) How do the polyene macrolide antibiotics affect the cellular membrane properties? Biochim Biophys Acta 864:257–304

Bolard J, Legrand P, Heitz F, Cybulska B (1991) One-side action of amphotericin B on cholesterol-containing membranes is determined by its self-association in the medium. Biochemistry 30:5707–5715

Bonilla-Marin M, Moreno-Bello M, Ortega-Blake I (1991) A microscopic electrostatic model for the amphotericin B channel. Biochim Biophys Acta 1061:65–77

Borisova MP, Brutyan RA, Ermishkin LN (1986) Mechanism of anion-cation selectivity of amphotericin B channels. J Membr Biol 90:13–20

Brajtburg J, Powderly WG, Kobayashi GS, Medoff G (1990) Amphotericin B: current understanding of mechanisms of action. Antimicrob Agents Chemother 34:183–188

Brooks BR, Bruccoleri RE, Olafson BD, States DJ, Swaminathan S, Karplus M (1983) Charmm: a program for macromolecular energy, minimization, and dynamics calculations. J Comput Chem 4:187–217

Brutyan RA, McPhie P (1996) On the one-sided action of amphotericin B on lipid bilayer membranes. J Gen Physiol 107:69–78

Chen D, Lear J, Eisenberg B (1997) Permeation through an open channel: Poisson-Nernst-Planck theory of a synthetic ionic channel. Biophys J 72:97–116

Chen WC, Bittman R (1977) Kinetics of association of amphotericin B with vesicles. Biochemistry 16:4145–4149

Cheng W, Wang CX, Chen WZ, Xu YW, Shi YY (1998) Investigating the dielectric effects of channel pore water on the electrostatic barriers of the permeation ion by the finite difference Poisson-Boltzmann method. Eur Biophys J 27:105–112

Clejan S, Bittman R (1985) Rates of amphotericin B and filipin association with sterols. A study of changes in sterol structure and phospholipid composition of vesicles. J Biol Chem 260:2884–2889

Cybulska B, Gadomska I, Mazerski J, Grzybowska J, Borowski E, Cheron M, Bolard J (2000) *N*-Methyl-*N*-D-fructosyl amphotericin B methyl ester (MF-AME), a novel antifungal agent of low toxicity: monomer/micelle control over selective toxicity. Acta Biochim Pol 47:121–131

De Kruijff B, Demel RA (1974) Polyene antibiotic-sterol interactions in membranes of acholeplasma laidlawii cells and lecithin liposomes. III. Molecular structure of the polyene antibiotic-cholesterol complexes. Biochim Biophys Acta 339:57–70

DiGiorgio AF, Otto S, Bandyopadhyay P, Regen SL (2000) Ion conductors that favor passive transport in ergosterol-rich over cholesterol-rich phospholipid membranes. J Am Chem Soc 122:11029–11030

Dufourc EJ, Smith JCP, Jarrell HD (1984) Amphotericin and model membranes. The effect of amphotericin B on cholesterol-containing systems as viewed by ^{2}H-NMR. Biochim Biophys Acta 776:317–329

Eisenberg RS (1996) Computing the field in proteins and channels. J Membr Biol 150:1–25

Fournier I, Barwicz J, Tancrede P (1998) The structuring effects of amphotericin B on pure and ergosterol- or cholesterol-containing dipalmitoylphosphatidylcholine bilayers: a differential scanning calorimetry study. Biochim Biophys Acta 1373:76–86

Friedman HL (1986) A course in statistical mechanics. Prentice-Hall, Englewood Cliffs, NJ

Fujii G, Chang JE, Coley T, Steere B (1997) The formation of amphotericin B ion channels in lipid bilayers. Biochemistry 36:4959–4968

Gallis HA, Drew RH, Pickard WW (1990) Amphotericin B: 30 years of clinical experience. Rev Infect Dis 12:308–329

Ganis P, Avitabile G, Mechlinski W, Schaffner CP (1971) Polyene macrolide antibiotic amphotericin B. Crystal structure of the *N*-iodoacetyl derivative. J Am Chem Soc 93:4560–4564

Gruda I, Bolard J (1987) On the existence of an amphotericin B-sterol complex in lipid vesicles and in propanol-water systems. Biochem Cell Biol 65:234–238

Gruda I, Nadeau P, Brajtburg J, Medoff G (1980) Application of differential spectra in the ultraviolet-visible region to study the formation of amphotericin B-sterol complexes. Biochim Biophys Acta 602:260–268

Grzybowska J, Sowinski P, Gumieniak J, Zieniawa T, Borowski E (1997) *N*-Methyl-*N*-D-fructopyranosylamphotericin B methyl ester, a new amphotericin B derivative of low toxicity. J Antibiot 50:709–711

Hartsel S, Bolard J (1996) Amphotericin B: new life for an old drug. Trends Pharmacol Sci 17:445–449

Hartsel SC, Benz SK, Peteron RP, Whyte BS (1991) Potassium-selective amphotericin B channels are predominant in vesicles regardless of sidedness. Biochemistry 30:77–82

Hartsel SC, Hatch C, Ayenew W (1993) How does amphotericin B work? Studies on model membrane systems. J Liposome Res 3:377–408

Hartsel SC, Benz SK, Ayenew W, Bolard J (1994) Na^{+}, K^{+} and Cl^{-} selectivity of the permeability pathways induced through sterol-containing membrane vesicles by amphotericin B and other polyene antibiotics. Eur Biophys J 23:125–132

Herve M, Debouzy JC, Borowski E, Cybulska B, Gary-Bobo CM (1989) The role of the carboxyl and amino groups of polyene macrolides in their interactions with sterols and their selective toxicity. A ^{31}P-NMR study. Biochim Biophys Acta 980:261–272

Hille B (1992) Ionic channels of excitable membranes. Sinauer Associates, Sunderland, Massachusetts

Holz R, Finkelstein A (1970) The water and nonelectrolyte permeability induced in thin lipid membranes by the polyene antibiotics nystatin and amphotericin B. J Gen Physiol 125:145

Hull SE, Woolfson MM (1976) The crystal structure of ergosterol monohydrate. Acta Crystallogr Sect B 32:2370–2373

Im W, Seefeld S, Roux B (2000) A grand canonical Monte Carlo-Brownian dynamics algorithm for simulating ion channels. Biophys J 79:788–801

Joly V, Bolard J, Saint Julien L, Carbon C, Yeni P (1992) Influence of phospholipid/amphotericin B ratio and phospholipid type on in vitro renal cell toxicities and fungicidal activities of lipid-associated amphotericin B formulations. Antimicrob Agents Chemother 36:262–266

Jordan PC, Bacquet RJ, McCammon JA, Tran P (1989) How electrolyte shielding influences the electrical potential in transmembrane ion channels. Biophys J 55:1041–1052

Jullien S, Brajtburg J, Bolard J (1990) Affinity of amphotericin B for phosphatidylcholine vesicles as a determinant of the in vitro cellular toxicity of liposomal preparations. Biochim Biophys Acta 1021:39–45

Kasumov KM, Borisova MP, Ermishkin LN, Potseluyev VM, Silberstein AY, Vainshtein VA (1979) How do ionic channel properties depend on the structure of polyene antibiotic molecules? Biochim Biophys Acta 551:229–237

Khutorsky VE (1992) Structures of amphotericin B-cholesterol complex. Biochim Biophys Acta 1108:123–127

Khutorsky V (1996) Ion coordination in the amphotericin B channel. Biophys J 71:2984–2995

Kleinberg ME, Finkelstein A (1984) Single-length and double-length channels formed by nystatin in lipid bilayer membranes. J Membr Biol 80:257–269

Kotler-Brajtburg J, Price HD, Medoff G, Schlessinger D, Kobayashi GS (1974) Molecular basis for the selective toxicity of amphotericin B for yeast and filipin for animal cells. Antimicrob Agents Chemother 5:377–382

Kuyucak S, Hoyles M, Chung SH (1998) Analytical solutions of Poisson's equation for realistic geometrical shapes of membrane ion channels. Biophys J 74:22–36

Laio A, Torre V (1999) Physical origin of selectivity in ionic channels of biological membranes. Biophys J 76:129–148
Langlet J, Berges J, Caillet J, Demaret JP (1994) Theoretical study of the complexation of amphotericin B with sterols. Biochim Biophys Acta 1191:79–93
Levitt DG (1999) Perspective – modeling of ion channels. J Gen Physiol 113:789–794
Madura JD, Briggs JM, Wade RC, Davis ME, Luty BA, Ilin A, Antosiewicz J, Gilson MK, Bagheri B, Scott LR, McCammon JA (1995) Electrostatics and diffusion of molecules in solution: simulations with the University of Houston Brownian dynamics program. Comput Phys Commun 91:57–95
Marty A, Finkelstein A (1975) Pores formed in lipid bilayer membranes by nystatin. Differences in its one-sided and two-sided action. J Gen Physiol 65:515–526
McGill P, Schumaker MF (1996) Boundary conditions for single-ion diffusion. Biophys J 71:1723–1742
Medoff G, Brajtburg J, Kobayashi GS, Bolard J (1983) Antifungal agents useful in therapy of systemic fungal infections. Annu Rev Pharmacol Toxicol 23:303–330
Mickus DE, Levitt DG, Rychnovsky SD (1992) Enantiomeric cholesterol as a probe of ion-channel structure. J Am Chem Soc 114:359–360
Partenskii MB, Jordan PC (1992) Theoretical perspectives on ion-channel electrostatics – continuum and microscopic approaches. Q Rev Biophys 25:477–510
Pratt LR, Hummer G, Garcia AE (1994) Ion pair potentials-of-mean-force in water. Biophys Chem 51:147–165
Ranatunga KM, Adcock C, Kerr ID, Smith GR, Sansom MSP (1999) Ion channels of biological membranes: prediction of single channel conductance. Theor Chem Acc 101:97–102
Rashin AA (1989) Electrostatics of ion-ion interactions in solution. J Phys Chem 93:4664–4669
Resat H, Mezei M (1994) Grand canonical Monte Carlo simulations of water positions in crystal hydrates. J Am Chem Soc 116:7451–7452
Resat H, Marrone TJ, McCammon JA (1997) Enzyme-inhibitor association thermodynamics: explicit and continuum solvent studies. Biophys J 72:522–532
Resat H, Sungur FA, Baginski M, Borowski E, Aviyente V (2000) Conformational properties of amphotericin B amide derivatives – impact on selective toxicity. J Comput Aid Mol Des 14:689–703
Roux B (1997) Influence of the membrane potential on the free energy of an intrinsic protein. Biophys J 73:2980–2989
Roux B (1999) Statistical mechanical equilibrium theory of selective ion channels. Biophys J 77:139–153
Saka Y, Mita T (1998) Interaction of amphotericin B with cholesterol in monolayers, aqueous solutions, and phospholipid bilayers. J Biochem (Tokyo) 123:798–805
Sansom MSP (1998) Models and simulations of ion channels and related membrane proteins. Curr Opin Struct Biol 8:237–244
Sansom MSP, Smith GR, Adcock C, Biggin PC (1997) The dielectric properties of water within model transbilayer pores. Biophys J 73:2404–2415
Sansom MSP, Shrivastava IH, Ranatunga KM, Smith GR (2000) Simulations of ion channels – watching ions and water move. Trends Biochem Sci 25:368–374
Shieh HS, Hoard LG, Nordman CE (1981) The structure of cholesterol. Acta Crystallogr Sect B 37:1538–1543
Silberstein A (1998) Conformational analysis of amphotericin B-cholesterol channel complex. J Membr Biol 162:117–126
Sperelakis N (1995) Cell physiology source book. Academic Press, San Diego, pp 67–90
Szlinder-Richert J, Mazerski J, Cybulska B, Grzybowska J, Borowski E (2001) MFAME, *N*-methyl-*N*-D-fructosyl amphotericin B methyl ester, a new amphotericin B derivative of low toxicity: relationship between self-association and effects on red blood cells. Biochim Biophys Acta 1528:15–24
Teerlink T, De Kruijff B, Demel RA (1980) The action of pimaricin, etruscomycin and amphotericin B on liposomes with varying sterol content. Biochim Biophys Acta 599:484–492
Van Hoogevest P, De Kruijff B (1978) Effect of amphotericin B on cholesterol-containing liposomes of egg phosphatidylcholine and didocosenoyl phosphatidylcholine. A refinement of the model for the formation of pores by amphotericin B in membranes. Biochim Biophys Acta 511:397–407
Vertut-Croquin A, Bolard J, Chabbert M, Gary-Bobo CM (1983) Differences in the interaction of the polyene antibiotic amphotericin B with cholesterol- or ergosterol-containing phospholipid vesicles. A circular dichroism and permeability study. Biochemistry 22:2939–2944
Weakliem CL, Fujii G, Chang J, Ben-Shaul A, Gelbart WM (1995) Effect of tension on pore formation in drug-containing vesicles. J Am Chem Soc 99:7694–7697
Weetman P, Goldman S, Gray CG (1997) Use of the Poisson-Boltzmann equation to estimate the electrostatic free energy barrier for dielectric models of biological ion channels. J Phys Chem B 101:6073–6078
Whyte BS, Peterson RP, Hartsel SC (1989) Amphotericin B and nystatin show different activities on sterol-free vesicles. Biochem Biophys Res Commun 164:609–614
Wolf BD, Hartsel SC (1995) Osmotic stress sensitizes sterol-free phospholipid bilayers to the action of amphotericin B. Biochim Biophys Acta 1238:156–162
WongBeringer A, Jacobs RA, Guglielmo BJ (1998) Lipid formulations of amphotericin B: clinical efficacy and toxicities. Clin Infect Dis 27:603–618
Woolf TB, Roux B (1996) Structure, energetics, and dynamics of lipid-protein interactions: a molecular dynamics study of the gramicidin A channel in DMPC bilayer. Proteins Struct Funct Genet 24:92–114